DALTON

Synthesis, structural and magnetic characterisation of tris(1-methyl-4,5-diphenylimidazol-2-yl)methanol (L) and $[\{CuL(NO_3)\}_2][NO_3]_2$

Timothy C. Higgs,[a] Madeleine Helliwell,[a] Eric J. L. McInnes,[b] Frank E. Mabbs,[b] Charles J. Harding[c] and C. David Garner[a]

[a] *The Chemistry Department, University of Manchester, Oxford Road, Manchester M13 9PL, UK*
[b] *EPSRC c.w.EPR Service Centre, The Chemistry Department, University of Manchester, Oxford Road, Manchester M13 9PL, UK*
[c] *The Department of Chemistry, The Open University, Walton Hall, Milton Keynes MK7 6AA, UK*

Tris(1-methyl-4,5-diphenylimidazol-2-yl)methanol (L) has been synthesized and characterised. It crystallises as L·0.5 1,2-$Cl_2C_2H_4$ from 1,2-$Cl_2C_2H_4$–light petroleum and its crystal structure has been determined. This compound reacts with $Cu(NO_3)_2·3H_2O$ to yield $[\{CuL(NO_3)\}_2][NO_3]_2$ which has also been crystallographically characterised. Each $[\{CuL(NO_3)\}_2]^{2+}$ is located on a crystallographic inversion centre; the N_2O_3 co-ordination sphere has a geometry intermediate between square pyramidal and trigonal bipyramidal, with a slight bias towards the former. The Cu(1)–O(1)–Cu(1*) bridging angle is small at 95.1(2)° and the Cu · · · Cu separation of 3.011(1) Å is typical of a coplanar-type di-μ-oxo-copper(II) dimer. Magnetic susceptibility (300–4 K) measurements indicated that the dimeric complex has a spin-triplet ground state, *i.e.* the two copper(II) ions are ferromagnetically coupled. Variable-temperature (300–4 K) EPR spectroscopy confirmed an $S = 1$ ground state described by the spin-Hamiltonian parameters $g_{xx} = 2.09$, $g_{yy} = 2.08$, $g_{zz} = 2.24$, $|D| = 0.35$ cm^{-1} and $|E| = 0.049$ cm^{-1} at room temperature. The magnitude of the zero-field splitting parameter $|D|$ and the value of $2J$ decrease with decreasing temperature.

The structural and magnetic properties of numerous dinuclear $Cu^{II}_2O_2$-type complexes have been studied in order to ascertain the factors that influence the magnitude and type (ferro- or anti-ferromagnetic) of spin–spin exchange interactions. Many trends and relationships have been empirically deduced and theoretically interpreted.[1,2] Key features identified include: (*i*) the magnitude of the Cu–O–Cu bridging angle in di-μ-OH bridged copper(II) complexes;[3] (*ii*) the electron density on the bridging oxygen atoms in corresponding di-μ-OR systems;[4] (*iii*) the degree of tetrahedrality of the ligand stereochemistry about the metal atoms in four-co-ordinate copper(II) dimers;[5] (*iv*) the extent of the fold of the two CuO_2 planes about the μ-O · · · μ-O axis.[6]

As part of our investigations of the reactivity of copper with various bi-/tri-imidazole compounds,[7–9] the tri-imidazole ligand tris(1-methyl-4,5-diphenylimidazol-2-yl)methanol was synthesized. Its reaction with various copper(II) salts has resulted in the formation of several interesting polynuclear copper(II) species. Herein, we report the synthesis and characterisation of the pro-ligand L and its dinuclear copper(II) complex $[\{CuL(NO_3)\}_2][NO_3]_2$, including a study of its magnetic properties.

Experimental

Syntheses

Tris(1-methyl-4,5-diphenylimidazol-2-yl)methanol L. This is a relatively simple two-step synthesis (Scheme 1) based on the procedures developed by Breslow and co-workers[10,11] and Brown and Huguet.[12] However, whereas these workers produced tris(imidazol-2-yl)methanol compounds with unsubstituted imidazoles or alkyl (methyl, isopropyl) substitution on the 4 and 5 positions of the imidazoles, we considered it desirable to have the larger phenyl steric hindrance at these ring positions. The synthesis consisted of two reactions. First, imidazole N^1 protection, replacing the NH proton of 4,5-diphenylimidazole by methyl. Secondly, lithiation of the N-protected imidazole at the C^2 position with *n*-butyllithium, followed by reaction with one-third of an equivalent of diethyl carbonate to form tris(1-methyl-4,5-diphenylimidazol-2-yl)methanol.

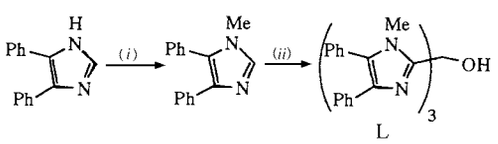

Scheme 1 (*i*) NaH, MeI, thf, argon; (*ii*) $LiBu^n$, $\frac{1}{3}OC(OEt)_2$, thf, argon

To a suspension of 4,5-diphenylimidazole (15.87 g, 0.072 mol) in dry, degassed tetrahydrofuran (thf) (100 cm^3) under an argon atmosphere was added NaH (80% dispersion in mineral oil, 3.24 g, 0.11 mol) in 0.25 g portions over 30 min. After the final addition the mixture was stirred for 30 min. Methyl iodide (4.9 cm^3, 0.079 mol) was added over 10 min during which time an exothermic reaction occurred. The sodium imidazolate dissolved, followed by the precipitation of a dense white solid (NaI). The mixture was stirred at room temperature for 2 h before the excess of NaH was quenched by careful dropwise addition of EtOH–Pr^iOH (2:1, 30 cm^3). The mixture was poured into water (500 cm^3), causing instant precipitation of product, and stirred vigorously for 10 min before the solid was filtered off and air dried. The crude product was dissolved in CH_2Cl_2 (200 cm^3) and dried over anhydrous $MgSO_4$. The $MgSO_4$ was removed and washed with CH_2Cl_2 (2 × 30 cm^3). The filtrate and washings were combined and toluene (50 cm^3) added to the solution. The CH_2Cl_2 component was removed under reduced pressure and the resultant yellow toluene solution allowed to cool to room temperature, resulting in the rapid precipitation of a microcrystalline white solid (1-methyl-4,5-diphenylimidazole) which was filtered off, washed with toluene (20 cm^3), Et_2O (30 cm^3) and dried *in vacuo*. Yield: 13.2 g (78%), m.p. 163–165 °C. ^{1}H NMR (200 MHz, $CDCl_3$): δ 3.5 (s, 3 H,

CH_3) and 7.1–7.6 (m, 11 H, aryl H) (Found: C, 81.8; H, 6.0; N, 12.0. Calc. for $C_{16}H_{14}N_2$: C, 82.0; H, 6.0; N, 12.0%). Chemical ionisation mass spectrum: *m/z* 235 (Calc.: M^+, $C_{16}H_{14}N_2$: 234).

A suspension of 1-methyl-4,5-diphenylimidazole (5.0 g, 0.021 mol) in dry, degassed thf (80 cm^3) was stirred for 5 min under an argon atmosphere until the solid had dissolved. The colourless solution was cooled to −78 °C and LiBu^n (1.6 mol dm^{-3} in hexane, 13.3 cm^3, 0.021 mol) added dropwise over 10 min. The mixture was stirred for 1 h at −78 °C to give a red-brown solution. After addition of dry, degassed diethyl carbonate (0.83 cm^3, 0.0069 mol) the solution was allowed to warm to room temperature over 2 h and stirred for 90 min, during which time it changed to an intense red. The reaction was quenched by addition of water (2 × 20 cm^3) causing an instant change to pale yellow. The thf component was removed under reduced pressure yielding a sticky yellow solid in the residual water. The aqueous layer was removed by decantation and the yellow solid dissolved in CH_2Cl_2 (100 cm^3) and dried over anhydrous $MgSO_4$. The $MgSO_4$ was removed and washed with two portions of CH_2Cl_2 (20 cm^3). The filtrate and washings were combined and reduced to a volume of 30 cm^3 under reduced pressure. Absolute EtOH (25 cm^3) was added and the solvent allowed to evaporate over several days causing the precipitation of a pale yellow solid. Recrystallisation from absolute EtOH–CH_2Cl_2 (1:3) yielded a white crystalline solid which was filtered off, washed with absolute EtOH (10 cm^3), Et_2O (20 cm^3) and dried *in vacuo*. Yield: 3.9 g (78%), m.p. 222–224 °C. ^{1}H NMR (300 MHz, $CDCl_3$): δ 3.5 (s, 9 H, CH_3), 6.7 (s, 1 H, OH) and 7.1–7.7 (m, 36 H, aryl H) (Found: C, 80.5; H, 5.6; N, 11.4. Calc. for $C_{49}H_{40}N_6O$: C, 80.8; H, 5.5; N, 11.5%). Fast atom bombardment mass spectrum: *m/z* 730 (Calc.: M^+, $C_{49}H_{40}N_6O$: 728).

[{CuL(NO$_3$)}$_2$][NO$_3$]$_2$. The salt $Cu(NO_3)_2 \cdot 3H_2O$ (0.063 g, 2.48×10^{-4} mol) was added to a solution of L (0.20 g, 2.75×10^{-4} mol) in CH_2Cl_2 (30 cm^3)–absolute EtOH (20 cm^3) and stirred for 10 min at room temperature to give a green solution. Toluene (20 cm^3) was added and the CH_2Cl_2–absolute EtOH was evaporated under reduced pressure causing the precipitation of a pale green microcrystalline solid which was filtered off, washed with toluene (5 cm^3), Et_2O (5 cm^3) and dried *in vacuo*. Yield: 0.19 g (84%) (Found: C, 64.2; H, 4.7; Cu, 6.6; N, 12.2. Calc. for $C_{49}H_{40}CuN_8O_7$: C, 64.2; H, 4.4; Cu, 6.9; N, 12.2%). FAB mass spectrum: *m/z* (proposed fragment) 918 {$[Cu_2L(NO_3)]^+$}, 854 ($[Cu_2L]^+$), 792 ($[CuL]^+$) and 712 ($[L - Me]^+$).

Physical measurements

The NMR spectra were recorded using a Varian Gemini 200 spectrometer or a Bruker AC300 spectrometer, chemical ionisation mass spectra using an IC Kratos MC 25 instrument, FAB spectra using a Kratos Concept 1S spectrometer, EPR spectra at X- (*ca.* 9.5) K- (*ca.* 24.2) and Q-band (*ca.* 34.2 GHz) frequencies on a Bruker ESP300E spectrometer. X-Band measurements from 300 to 100 K utilised a Bruker ER4116DM resonator with a BVT2000 variable-temperature unit; an Oxford Instruments ESR910 cryostat was used for temperatures below 100 K. An ER6706KT and an ER5106QT resonator were used for K- and Q-band measurements, respectively, with cooling *via* either an ER4118VT (300–100 K) or an ER4118CF (100–4.2 K) cryostat. Computer simulations of spectra were achieved *via* in-house software.[13] The variable-temperature magnetic susceptibility studies on $[\{CuL(NO_3)\}_2][NO_3]_2$ were made using an Oxford Instruments Faraday susceptibility balance, with an electromagnet operating at 8000 G (0.8 T); the data were collected from 4 to 300 K at 10 K intervals above 30 K and at closer intervals at lower temperature, each data point being the average of 36 measurements. A correction was made for the measured diamagnetism of the Teflon sample container. The molar susceptibility was corrected for the diamagnetic contribution of the sample using Pascal constants.

Crystallography

A summary of the key crystallographic information is given in Table 1. All intensity data were corrected for Lorentz-polarisation, and absorption effects using the program DIFABS.[14] During data collection for each crystal the intensities of three representative reflections were measured every 150; for L·0.5 1,2-$Cl_2C_2H_4$ these declined by 5.4% and for $[\{CuL(NO_3)\}_2][NO_3]_2 \cdot$ 4thf a reduction in intensity of 5.6% was observed; a linear correction factor was applied to the sets of data to account for these decays. The structure of L·0.5 1,2-$Cl_2C_2H_4$, was solved by direct methods using the programs MITHRIL[15] and DIRDIF,[16] and that of $[\{CuL(NO_3)\}_2][NO_3]_2 \cdot$4thf by Patterson methods using the software SHELXS 86[17] and DIRDIF.[16] In each case the function minimised during full-matrix, least-squares refinement was $\Sigma w(|F_o| - |F_c|)^2$ using standard neutral-atom scattering factors and anomalous dispersion corrections.[18]

L·0.5 1,2-Cl$_2$C$_2$H$_4$. Crystals were grown by solvent layering in a sealed Pasteur pipette, with a 1,2-$Cl_2C_2H_4$ solution of the compound and light petroleum (b.p. 60–80 °C) as the counter solvent. The colourless block shaped crystals were sensitive to loss of solvent upon removal from the mother-liquor. Consequently, the crystal used in the crystallographic investigation was mounted in a glass capillary, together with some of its mother-liquor. The non-hydrogen atoms of the molecule were refined anisotropically. Half a molecule of the solvent, 1,2-$Cl_2C_2H_4$, was located by Fourier-difference techniques. Hydrogen atoms attached to carbon were included in the structure-factor calculation in idealised positions (C–H 0.95 Å) and assigned isotropic thermal parameters 20% larger than the equivalent *B* value of the atom to which they were bonded. The H(1) atom bonded to O(1) was located by Fourier-difference methods. The maximum and minimum peaks on the final Fourier-difference map corresponded to 0.50 and −0.49 e $Å^{-3}$, respectively.

[{CuL(NO$_3$)}$_2$][NO$_3$]$_2$·4thf. Crystals were grown by solvent layering. A solution of the compound was prepared in CH_2Cl_2 and then transferred to a Pasteur pipette (flame sealed at one end). Five times the volume of thf was then carefully layered onto the CH_2Cl_2 solution and the pipette completely sealed. Over several days small green, block-like crystals formed. One was mounted on a glass fibre. The asymmetric unit contained half the formula weight of the compound (the other half being generated by inversion through the centre of symmetry). Three disordered fragments were also located; the first was assumed to be a nitrate anion with six positions for oxygen, three at an occupancy of 0.6, the other three at an occupancy of 0.4; the other two fragments were considered to be thf (for one molecule only four non-hydrogen atoms were located whilst for the other five non-hydrogen atoms were found); however, it was not possible to ascertain which of these atoms were oxygen, and so all were refined as carbon. The non-hydrogen atoms were refined anisotropically, except for N(8) and the atoms of the two thf fragments which were refined isotropically. Hydrogen atoms were included in the structure-factor calculation in idealised positions (C–H 0.95 Å) and were assigned isotropic thermal parameters that were 20% larger than the equivalent *B* value of the atom to which they were bound. The hydrogen atoms of the thf fragments were not included. The maximum and minimum peaks on the final Fourier-difference map corresponded to 0.81 and −0.66 e $Å^{-3}$, respectively. The disorder and other uncertainties noted above resulted in the final *R* and *R′* values, 0.084 and 0.101, being larger than usual.

Atomic coordinates, thermal parameters, and bond lengths and angles have been deposited at the Cambridge Crystallographic Data Centre (CCDC). See Instructions for Authors, *J. Chem. Soc., Dalton Trans.*, 1997, Issue 1. Any request to the CCDC for this material should quote the full literature citation and the reference number 186/391.

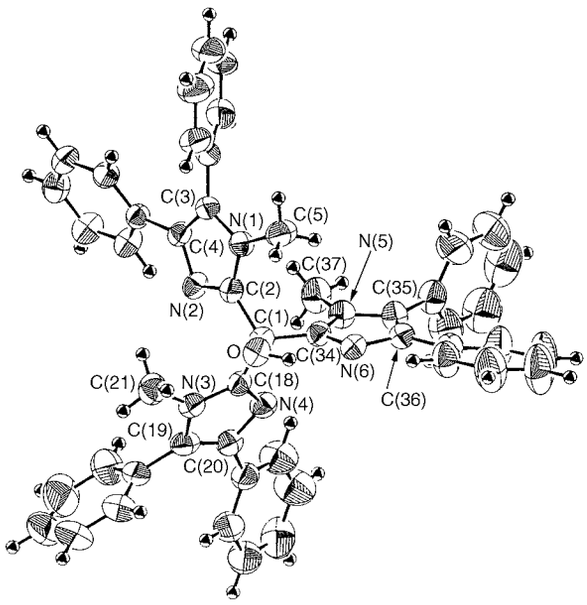

Fig. 1 An ORTEP[19] view of the L molecule showing the atom numbering scheme

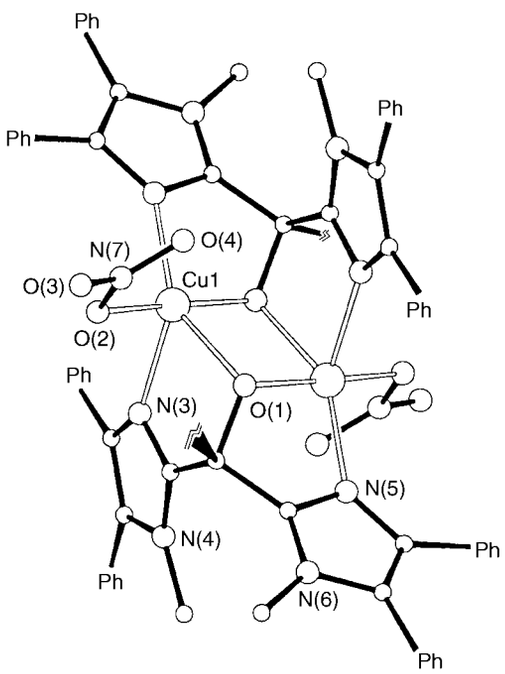

Fig. 2 Schematic view of the structure of $[\{CuL(NO_3)\}_2]^{2+}$

Results and Discussion

Crystal structures

L·0.5 1,2-$Cl_2C_2H_4$. The crystal structure of L·0.5 1,2-$Cl_2C_2H_4$ consists of L (Fig. 1) and a molecule of 1,2-$Cl_2C_2H_4$ disordered over two sites which are related by a centre of symmetry. The molecular structure confirms that the synthesis has progressed successfully, and that for any two of the imidazole rings of this pro-ligand to bind to a single metal atom will require considerable reorientation of the relevant heterocyclic rings.

$[\{CuL(NO_3)\}_2][NO_3]_2$·4thf. The structure consists of centrosymmetric dimeric copper cations (Fig. 2). There are also two non-bonded nitrate anions (>3.60 Å from any Cu^{II}) per $[\{CuL(NO_3)\}_2]^{2+}$ cation, and four non-bonded thf solvent molecules in the lattice. Each $[\{CuL(NO_3)\}_2]^{2+}$ cation contains two copper(II) ions bound together by two bridging systems: the carbinol oxygens in a di-μ-O(H)R fashion and two imidazoles of each L; one imidazole co-ordinates to one metal ion and the other to the second metal ion. The alcohol oxygens are not considered to be deprotonated according to the analytical data (see above) which show two nitrates per Cu and a ratio Cu : L : NO_3 of 1 : 1 : 2. The EPR spectra and magnetic properties of the compound (see below) are all clearly indicative of a dimeric copper(II) system. Thus, Cu^{II}, $2NO_3^-$, plus neutral L gives a balancing of charges, but we cannot exclude the possibility of the proton of the carbinol being located elsewhere, *e.g.* on the unbound imidazole ring. However, there is no evidence for such proton transfer and the structure of the carbinol oxygen favours protonation with the bond angles about these atoms [Cu(1)–O(1)–Cu(1*) 95.1(2), Cu(1)–O(1)–C(1) 115.5(5), Cu(1*)–O(1)–C(1) 108.7(5)°, total = 319.3°, average = 106.4°] having values more compatible with sp^3 rather than sp^2 hybridisation at the oxygen. The Cu(1), O(1), Cu(1*), O(1*) atoms are crystallographically planar. In addition to the two μ-O(H)R and two imidazole groups, the Cu^{II} is co-ordinated to a unidentate[20] nitrato group through oxygen O(2). Thus, each Cu^{II} ion has an N_2O_3 co-ordination sphere. The third imidazole of each tris(imidazole) ligand remains non-co-ordinated.

Tables 2 and 3 list bond lengths and interbond angles. The structure of the $[\{CuL(NO_3)\}_2]^{2+}$ cation is greatly influenced by the nature of L (see Fig. 2); the steric hindrance imposed by the 4-Ph groups restricts co-ordination at each Cu^{II} and the bridging of the two metal centres is *via* two μ-OH groups, one from

Table 1 Crystal and refinement data* for the L·0.5 1,2-$Cl_2C_2H_4$ and $[\{CuL(NO_3)\}_2][NO_3]_2$·4thf

	L·0.5 1,2-$Cl_2C_2H_4$	$[\{CuL(NO_3)\}_2][NO_3]_2$·4thf
Formula	$C_{50}H_{44}ClN_6O$	$C_{57}H_{55}CuN_8O_9$
M	780.39	1059.66
a/Å	14.229(2)	14.124(3)
b/Å	14.283(4)	14.972(2)
c/Å	11.122(2)	13.026(2)
α/°	103.53(2)	91.15(1)
β/°	93.89(1)	93.87(2)
γ/°	81.17(2)	99.15(2)
U/Å^3	2170.3(9)	2711.9(8)
D_c/g cm^{-3}	1.194	1.298
F(000)	822	1108
Crystal size/mm	0.25 × 0.25 × 0.40	0.10 × 0.10 × 0.10
μ/cm^{-1}	11.02	10.50
T/ °C	22 ± 1	30 ± 1
$2\theta_{max}$/°	120.2	120.3
Total reflections	6756	8441
Unique reflections	6453	8060
Structure solution	Direct methods	Patterson
No. data used in refinement	3099	4486
Final R	0.071	0.084
Final R'	0.079	0.101

* Details in common: triclinic, space group $P\bar{1}$; $Z = 2$; Rigaku AFC5R diffractometer; graphite-monochromated Cu-Kα radiation (λ = 1.541 78 Å); ω–2θ scans; scan rate 8.0° min^{-1} in ω (two and three rescans); scan width 1.10 + 0.30 tan θ; $w = 1/[\sigma^2(F_o) + 0.0022|F_o|^2]$.

Table 2 Dimensions (bond lengths in Å, angles in °) of the copper(II) co-ordination sphere of $[\{CuL(NO_3)\}_2][NO_3]_2$ with estimated standard deviation (e.s.d.s) in parentheses

Cu(1)–O(1)	2.123(6)	Cu(1)–N(3)	2.158(7)
Cu(1)–O(1*)	1.955(5)	Cu(1)–N(5)	2.052(7)
Cu(1)–O(2)(NO_3)	1.934(6)	Cu(1)–O(4)(NO_3)	2.721(5)
O(1)–Cu(1)–O(1)	84.9(2)	O(1)–Cu(1)–N(5)	83.3(2)
O(1)–Cu(1)–O(2)	90.6(2)	O(2)–Cu(1)–N(3)	93.9(3)
O(1)–Cu(1)–N(3)	76.5(2)	O(2)–Cu(1)–N(5)	99.3(3)
O(1)–Cu(1)–N(5)	148.3(2)	N(3)–Cu(1)–N(5)	132.0(3)
O(1)–Cu(1)–O(2)	174.8(3)	Cu(1)–O(1)–Cu(1*)	95.1(2)
O(1)–Cu(1)–N(3)	87.6(2)		

each ligand. The nature of the five-co-ordinate geometry about Cu^{II} can be assessed using the structural index parameter $\tau = (\beta - \alpha)/60$, where β,α are the two largest co-ordination angles; $\tau = 0$ for square-pyramidal geometry and 1 for trigonal-bipyramidal geometry.[21] The value of τ in $[\{CuL(NO_3)\}_2]^{2+}$ is 0.442, indicating that the geometry is midway between trigonal bipyramidal and square pyramidal but with a slight bias towards the latter. With respect to a square-pyramidal geometry, the O(1), O(1*), O(2) and N(5) atoms would be considered as defining the basal plane; N(5) occupies a position considerably out of the O(1), O(1*), O(2) plane, indicative of a distortion towards a trigonal-bipyramidal geometry where N(5), N(3) and O(1) define the equatorial plane and O(1*) and O(2) occupy the axial positions.

Table 4 compares the Cu–O–Cu bond angles, the Cu–(μ-O) bond lengths, and the structural index parameters, τ, for the copper(II) centres of $[\{CuL(NO_3)\}_2][NO_3]_2$ with those of a number of related di-μ-O copper(II) dimers, where the metal centres are five-co-ordinate. In such systems the bridging modes are often described as being 'parallel planar' or 'coplanar' in relation to idealised trigonal-bipyramidal and square-pyramidal geometries, respectively (Fig. 3). The Cu···Cu separation of 3.011(1) Å in $[\{CuL(NO_3)\}_2][NO_3]_2$ compares favourably with those of previously reported coplanar CuO_2Cu centres (*ca.* 3.0 Å), whereas this distance is considerably shorter than the Cu···Cu separation of the parallel planar copper(II) dimers (by at least *ca.* 0.3 Å). The Cu···Cu separation thus implies that the bridging mode adopted by $[\{CuL(NO_3)\}_2][NO_3]_2$ is best described as coplanar.

The level of geometric distortion away from square pyramidal towards trigonal bipyramidal, as demonstrated by the structural index, $\tau = 0.442$ for $[\{CuL(NO_3)\}_2][NO_3]_2$, is the highest observed in Table 4 for both copper(II) ions jointly, although one of the metal ions of the $[Cu_2(N_6O)(OH)][BF_4]_2$[22] system is more distorted towards trigonal bipyramidal with a τ value of 0.502 (see above). The Cu–O–Cu bridging angles of $[\{CuL(NO_3)\}_2][NO_3]_2$ [95.1(2)°] are the smallest in Table 4.

EPR Spectroscopy

The EPR spectrum of $[\{CuL(NO_3)\}_2][NO_3]_2$ in CH_2Cl_2–toluene frozen solution at 77 K indicated that the dimer had dissociated to produce monomeric copper(II) centres ($g_\perp = 2.017$, $g_\parallel = 2.272$, $A_\parallel = 158$ G). Therefore, all of the EPR studies were performed on undiluted solids.

Table 3 Methanol bridge and imidazole ring bond lengths (Å) and angles (°) (with e.s.d.s) for the L ligand in $[\{CuL(NO_3)\}_2][NO_3]_2$

Methanol bridge			
C(2)–C(1)–C(34)	111.8(5)	C(1)–O(1)	1.435(6)
C(2)–C(1)–C(18)	110.1(5)	C(1)–C(2)	1.515(8)
C(18)–C(1)–C(34)	109.6(5)	C(1)–C(18)	1.503(8)
C(2)–C(1)–O(1)	108.6(5)	C(1)–C(34)	1.512(8)
C(18)–C(1)–O(1)	109.6(5)		
C(34)–C(1)–O(1)	106.9(5)		
Imidazole 1			
C(2)–N(1)–C(3)	105.8(5)	C(2)–N(1)	1.364(7)
N(1)–C(3)–C(4)	106.5(5)	N(1)–C(3)	1.390(7)
C(3)–C(4)–N(2)	109.4(5)	C(3)–C(4)	1.361(8)
C(4)–N(2)–C(2)	106.1(5)	C(4)–N(2)	1.383(7)
N(2)–C(2)–N(1)	112.2(5)	N(2)–C(2)	1.305(7)
Imidazole 2			
C(18)–N(3)–C(19)	107.0(5)	C(18)–N(3)	1.364(7)
N(3)–C(19)–C(20)	105.3(6)	N(3)–C(19)	1.389(7)
C(19)–C(20)–N(4)	110.5(6)	C(19)–C(20)	1.363(8)
C(20)–N(4)–C(18)	105.3(5)	C(20)–N(4)	1.390(7)
N(4)–C(18)–N(3)	111.9(6)	N(4)–C(18)	1.310(7)
Imidazole 3			
C(34)–N(5)–C(35)	106.8(5)	C(34)–N(5)	1.353(7)
N(5)–C(35)–C(36)	107.3(6)	N(5)–C(35)	1.373(7)
C(35)–C(36)–N(6)	108.5(5)	C(35)–C(36)	1.355(8)
C(36)–N(6)–C(34)	106.0(5)	C(36)–N(6)	1.395(7)
N(6)–C(34)–N(5)	111.4(5)	N(6)–C(34)	1.317(7)

Table 4 Structural comparison of $[\{CuL(NO_3)\}_2][NO_3]_2$ with other dimeric copper(II) dimers with five-co-ordinate metal centres

			Cu–(μ-O)/Å		τ		
System*	Cu–O–Cu/°	Cu···Cu/Å	O(1)	O(2)	Cu(1)	Cu(2)	Comments on structure
$[\{CuL(NO_3)\}_2][NO_3]_2$	95.1(2)	3.011(1)	2.123(6)	1.955(5)	0.442	0.442	Coplanar
$[Cu(esal)NO_3]_2$[23]	101.1(1)	3.008(1)	1.968(3)	1.926(3)	0.045	0.045	Coplanar
$[(CuL^1)_2][ClO_4]_2$[24]	98.2(6)	2.929	1.916(6)	1.958(6)	0.427	0.427	Coplanar
$[Cu_2L^2(OH)][ClO_4]_2\cdot H_2O$[25]	100.0(3)	3.019(2)	1.958(6)	1.894(6)	0.087	0.052	Coplanar
	104.3(3)		1.983(6)	1.930(6)			
$[Cu_2L^3(OH)(ClO_4)_2]\cdot 2MeOH$[26]	96.9(4)	2.994(1)	2.001(6)	1.868(6)	0.197	0.197	Coplanar
	106.5(5)						
$[Cu_2L^4(OH)][ClO_4]_2$[27]	99.19(6)	2.947	1.938(1)	1.920(1)	0.123	0.140	Coplanar
	100.44(7)		1.933(1)	1.915(1)			
$[\{Cu(py)_2(dbcat)\}_2]$[28]	100.5(1)	3.021(1)	1.964(2)	1.966(2)	<0.1	<0.1	Coplanar
$[\{CuL^5(ClO_4)\}_2]$[29]	96.5(1)	2.911(2)	1.951(3)	1.950(3)	0.207	0.207	Coplanar
$[\{CuL^5(dmso)\}_2][ClO_4]_2$[29]	96.1(2)	2.887(2)	1.927(4)	1.955(4)	0.277	0.277	Coplanar
$[\{CuL^6(dmso)\}_2][ClO_4]_2$[29]	98.3(1)	2.966(1)	1.957(2)	1.964(1)	0.213	0.213	Coplanar
$[\{CuL^7(ClO_4)\}_2]$[29]	102.4(1)	2.995(1)	1.913(1)	1.929(1)	0.079	0.079	Coplanar
$[Cu_2L^8(OH)][BF_4]_2$[22]	103.6(3)	3.053(4)	1.942(6)	2.002(8)	0.502	0.218	Unsymmetrical Cu(1)
	101.9(4)		1.941(6)	1.927(8)			and Cu(2) geometries
$[Cu_2L^9_2(O_2CMe)_2]\cdot 2H_2O$[30]	98.1(3)	3.384(3)	1.960(8)	2.498(8)	0.040	0.040	Parallel planar
$[\{Cu(tsgly)_2(bipy)\}_2]\cdot 2H_2O$[31]	100.0	3.317(1)	2.350(3)	1.968(2)	0.068	0.068	Parallel planar
$[\{CuL^{10}(O_2CMe)\}_2]\cdot 2H_2O$[32]	101.3(4)	3.507(3)	1.973(10)	2.485(10)	0.005	0.023	Parallel planar
	103.0(4)						
$[\{CuL^{11}(O_2CMe)\}_2]$[33]	95.34(5)	3.305	1.955(1)	2.490(1)	0.054	0.054	Parallel planar

esal = *N*-Ethyl-2-hydroxybenzylideneaminate); tsgly = *N*-tosylglycinate monoanion (tosyl : 4-toluene-*p*-sulfonyl); bipy = 2,2′-bipyridine; dbcat = 3,5-di-*tert*-butylbenzene-1,2-diolate; L^1 = 4,6,6-trimethyl-3,7-diazanon-3-ene-1,9-diolate; L^2 = 2-[*N*-(3-dimethylaminopropyl)formimidoyl]-6-[*N*-(2-pyridylethyl)formimidoyl]-phenolate; L^3 = 2,6-bis[4-(benzimidazol-2-yl)-2-thiabutyl]-4-methylphenolate; L^4 = 2,6-bis[*N*-(2-pyridylmethyl)formidoyl]-4-methylphenolate; L^5 = 2-(1,3,5,7-tetraazabicyclo[3.3.1]nonan-3-yl)ethanolate; L^6 = 2-{7-(methoxymethyl)-1,3,5,7-tetraazabicyclo[3.3.1]nonan-3-yl}ethanolate; L^7 = 3-(1,3,5,7-tetraazabicyclo[3.3.1]nonan-3-yl)propanolate; L^8 = 2,6-bis{bis[2-(pyrazol-1-yl)ethyl]aminomethyl}-*p*-cresolate; L^9 = *N*-methyl-*N*′-(5-methoxysalicylidene)propane-1,3-diaminate; L^{10} = 6-amino-1-(2′-hydroxyphenyl)-3-methyl-4-azahept-2-en-1-onate; L^{11} = 7-amino-4-methyl-5-azahept-3-en-2-onate; py = pyridine; dmso = dimethyl sulfoxide.

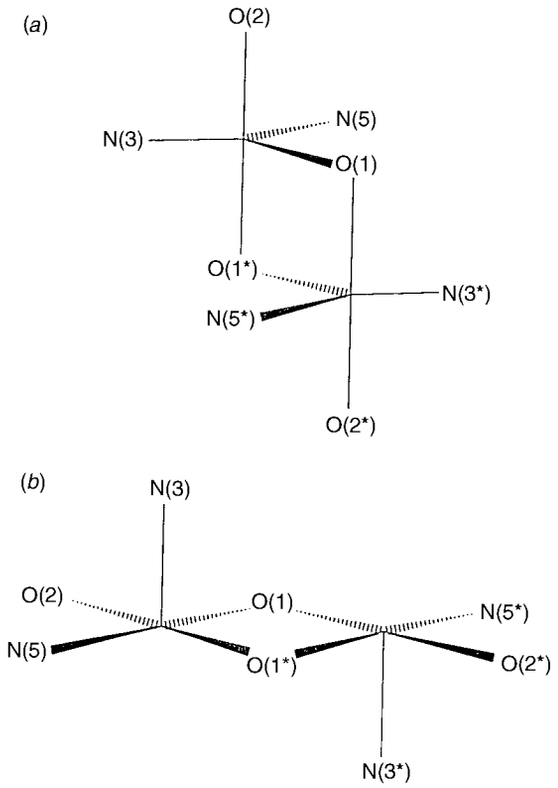

Fig. 3 Bridging modes of $[\{CuL(NO_3)\}_2]^{2+}$ with respect to the idealised geometries: (*a*) parallel planar (trigonal bipyramidal) and (*b*) coplanar bridging (square pyramidal)

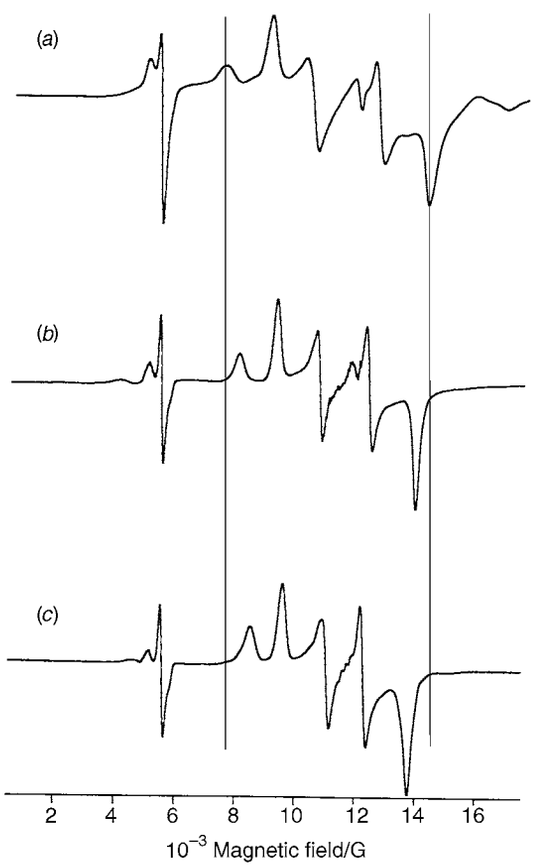

Fig. 4 Q-Band EPR spectra of $[\{CuL(NO_3)\}_2][NO_3]_2$ at (*a*) 300, (*b*) 160 K and (*c*) 4.2 K. The vertical lines are drawn to highlight the decreasing spread of the $|\Delta M_S| = 1$ resonances with temperature which shows that there is a decrease in the zero-field splitting

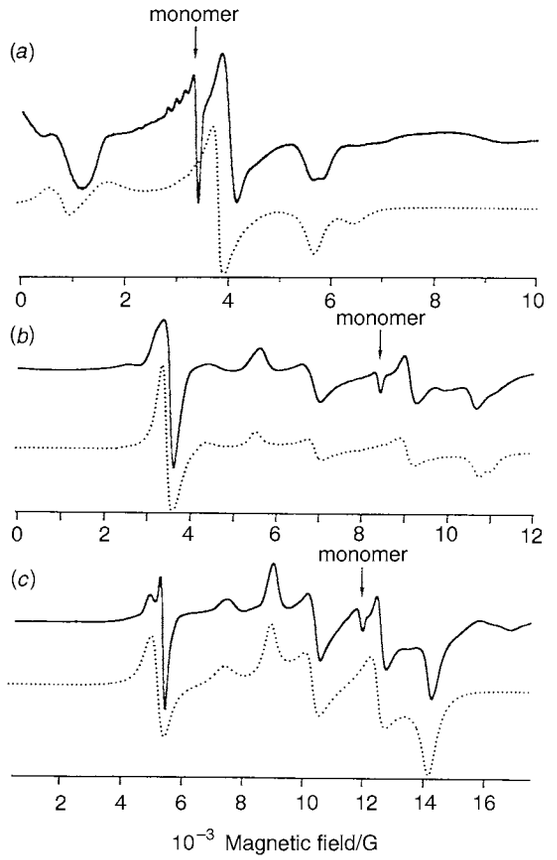

Fig. 5 (*a*) X-, (*b*) K- and (*c*) Q-band EPR spectra of $[\{CuL(NO_3)\}_2][NO_3]_2$ at 300 K (experimental, solid lines; simulated, dashed lines)

Powdered $[\{CuL(NO_3)\}_2][NO_3]_2$ was found to be EPR active at all temperatures (300–4.2 K) and frequencies (X-, K- and Q-band) studied. The spectra observed are consistnt with a spin-triplet state with both the usual $|\Delta M_S| = 1$ and 'half-field' $|\Delta M_S| = 2$ transitions. A monomeric impurity was also observed in all spectra which was less dominant at low temperatures. On cooling from 300 to 4.2 K two trends were observed. First, the total intensity of the triplet spectrum increased with decreasing temperature down to 4.2 K; this is consistent with a ferromagnetically exchange-coupled system as required by the magnetic susceptibility data, see below. Secondly, the spread of the $|\Delta M_S| = 1$ resonances decreased with decrease in temperature down to about 60 K (Fig. 4). Below this temperature the spectra did not change, except for small variations in linewidth. The room-temperature spectra at X-, K- and Q-band were simulated successfully with the spin-Hamiltonian parameters $g_{xx} = 2.09$, $g_{yy} = 2.08$, $g_{zz} = 2.24$ ($g_{av} = 2.14$), $|D| = 0.35$ cm^{-1} and $|E| = 0.049$ cm^{-1} with Lorentzian linewidths of 200–300 G, where D and E are the zero-field splitting parameters. The room-temperature X-, K- and Q-band EPR spectra and their simulations are shown in Fig. 5. The ability to simulate the major features in the EPR spectra at each of these frequencies with the *same* set of g, $|D|$ and $|E|$ values confirms their reliability. It should be noticed that there are certain features in the experimental spectra that could not be reproduced in the simulations [*e.g.* the low-field shoulder on the half-field transition at Q-band, Fig. 5(*c*)]. The origin of these 'extra' features is unclear, although the possibility of dimeric impurities cannot be ruled out. The experimentally observed zero-field splitting, D^{obs}, is the sum of the contributions from dipolar and anisotropic exchange interactions, D^{dip} and D^{exch}, respectively. The dipolar contribution can be estimated from the Cu···Cu distance.[34] The experimental Cu···Cu distances and g values give $D^{dip} = -0.11$ cm^{-1} at room temperature, a value much smaller than the experimentally observed $|D^{obs}| = 0.35$ cm^{-1}. Thus, the

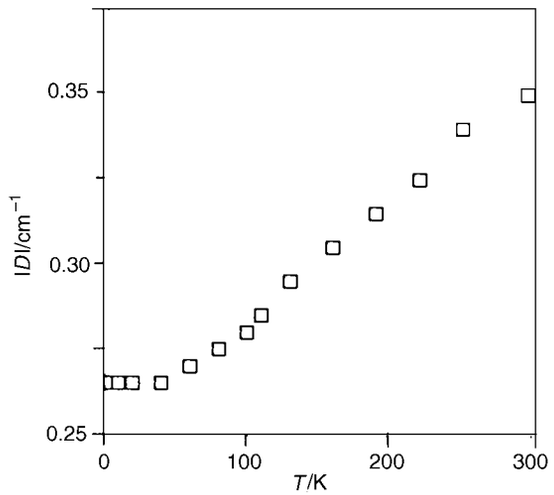

Fig. 6 Plot of $|D|$ *versus* T for $[\{CuL(NO_3)\}_2][NO_3]_2$

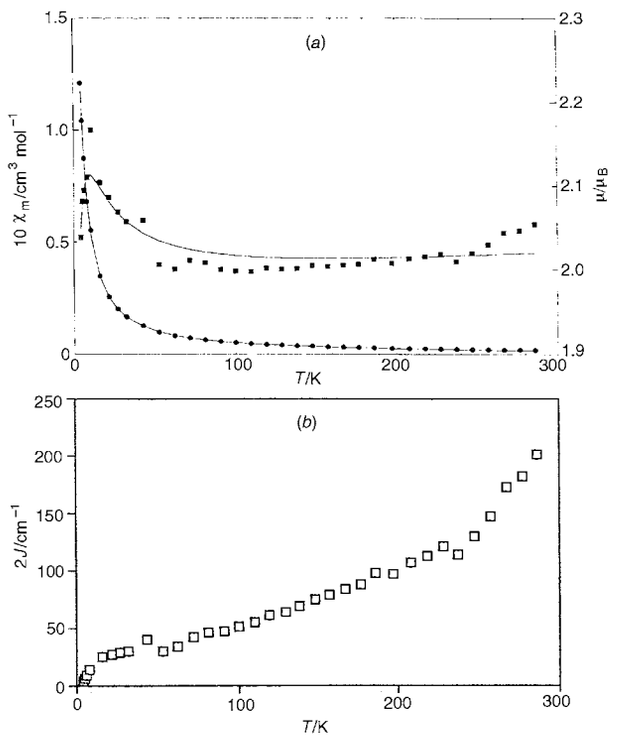

Fig. 7 (*a*) Plots of μ (■) and χ_m (●) *versus* T for $[\{CuL(NO_3)\}_2][NO_3]_2$; solid lines represent the best fits using equation (2) with $g = 2.28$, $2J = +12$ cm^{-1}, $\theta = -1$ K and $N\alpha = 60 \times 10^{-6}$ cm^3 mol^{-1} ($\mu_B \approx 9.274 \times 10^{-24}$ J T^{-1}). (*b*) The temperature variation of $2J$ calculated from equation (2) and the experimental χ_m with $g = 2.14$, $N\alpha = 60 \times 10^{-6}$ cm^3 mol^{-1} and $\theta = 0$

predominant contribution to the observed zero-field splitting is the anisotropic exchange interaction which results from the combined interactions of spin–orbit coupling and exchange in the excited states.

The changes in the EPR spectra on cooling arise from a decrease of the zero-field splitting, D. A plot of $|D|$ (from simulation of Q-band spectra) *versus* temperature reveals the decrease of $|D|$ down to *ca.* 60 K whereupon it levels out (Fig. 6). It is interesting that although $|D|$ decreases from 0.35 cm^{-1} at 300 K to 0.265 cm^{-1} at ≤60 K, $|E|$ remains within the narrow range of 0.049 ± 0.002 cm^{-1} and the g values are unchanged. The change in $|D|$ is reversible, *i.e.* on warming a sample from 4.2 to 300 K the original spectra were restored. The behaviour of $|D|$ and $2J$ (see below) implies that the exchange interaction varies with temperature. Changes in $|D|$ and $2J$ most likely result from small changes in structure with temperature, although in the absence of structural data at more than one temperature it is hard to be specific.

Variable-temperature magnetic susceptibility measurements

The variable-temperature magnetic susceptibility data in the range 4–290 K for $[\{CuL(NO_3)\}_2][NO_3]_2$ [Fig. 7(*a*)] do not exhibit a maximum suggesting that the interaction between the two copper(II) ions of the cation is ferromagnetic. This exchange interaction can be expressed by the exchange Hamiltonian (1),

$$H_{ex} = -2J\hat{S}_1 \cdot \hat{S}_2 \qquad (1)$$

where $2J$ is the single–triplet splitting; in this definition, a positive value of $2J$ represents a ferromagnetic interaction. The value of $2J$ is usually determined by fitting variable-temperature (300–4 K) susceptibility data for a polycrystalline sample by use of the Bleaney–Bowers equation (2),[35] where χ_m

$$\chi_m = [g^2\beta^2 N/3k_B(T - \theta)][1 + \tfrac{1}{3}\exp(-2J/k_B T)]^{-1} + N\alpha \quad (2)$$

is the molar susceptibility, T the temperature, θ the Weiss temperature, g the average g value, k_B the Boltzmann constant, β the Bohr magneton, and $N\alpha$ the temperature-independent paramagnetism. When the data in Fig. 7(*a*) were fitted using equation (2), by minimising the value of r in equation (3) and

$$r = \Sigma[\chi(\text{exptl}) - \chi(\text{theory})]^2/\Sigma[\chi(\text{exptl})]^2 \qquad (3)$$

allowing g, $2J$ and θ to vary, the magnetic parameters obtained were $g = 2.28$, $2J = +12$ cm^{-1} and $\theta = -1$ K ($N\alpha$ was set at 60×10^{-6} cm^3 mol^{-1} the accepted value per Cu^{II}). The best-fit value of g is inconsistent with the value of 2.14 obtained experimentally (see above). An attempt to model the magnetic data using the average g value of 2.14 determined from EPR measurements, but allowing all other parameters in equation (2) to vary, resulted in a much poorer fit between calculated and observed susceptibilities. We observed that the g value from the EPR spectra remained constant with temperature. By using the experimental g_{av} value, fixing $N\alpha = 60 \times 10^{-6}$ cm^3 mol^{-1} and $\theta = 0$, values of $2J$ can be calculated from equation (2) using the experimental susceptibilities. The result of this is shown in Fig. 7(*b*). The values of $2J$ are positive showing ferromagnetic coupling. However, $2J$ varies from 200 cm^{-1} at 290 K to 30 cm^{-1} at 50 K in an almost linear manner. Below about 20 K the value of $2J$ decreases more sharply. Apart from the fall in $2J$ below *ca.* 20 K, the temperature variation in $2J$ is similar to that of the zero-field splitting parameter, $|D|$, in the EPR spectra.

A major factor in determining the degree and type of spin coupling in di-μ-O bridged copper(II) dimers is the Cu–O–Cu bridge angle. In the classic study of Hatfield and co-workers[3] it was shown that for a series of bis(diamine)bis(μ-hydroxo)-copper(II) complexes the singlet–triplet splitting varied as a linear function of the Cu–O–Cu bridging angle. All of these complexes involved an essentially planar $N_2CuO_2CuN_2$ moiety, with Cu–O distances of 1.92 ± 0.03 Å and Cu–N distances of 2.00 ± 0.003 Å, with co-ordinated water molecules or counter ions in some cases. The Cu–O–Cu bond angles (φ) in these compounds range from 95.6(1) to 104.1(2)° and the singlet–triplet splitting varied linearly from +172 to −509 cm^{-1}, the linear relationship being described by equation (4). This

$$2J = -74.53\varphi + 7270 \text{ cm}^{-1} \qquad (4)$$

linear relationship leads to $2J = 0$ at Cu–O–Cu 97.5°.[3] In a similar study using a series of tetrameric copper(II) complexes with bridging *N*,*N*-dialkylated aminoalcohol ligands, where the tetramers behave as two non-interacting dimeric units,[36] a linear relationship (5) was established with $2J = 0$ at 95.7°. Substitution

$$2J = -82.1\varphi + 7857\ cm^{-1} \quad (5)$$

of the Cu–O–Cu bridging angle of $[\{CuL(NO_3)\}_2][NO_3]_2$ [φ = 95.1(2)°] into equations (4) and (5) leads to 2*J* values of +182 ± 45 and +49 ± 49 cm^{-1}, respectively. The value $2J = 200\ cm^{-1}$ at 290 K, a temperature close to that at which the structure was determined, is within the range obtained from equation (4).

Previous observations have shown that the nature of the bridging oxygen atoms in CuO_2Cu dimers can lead to significant deviations of 2*J* from those predicted by equation (4). For example, Hay *et al.*[2] concluded that an increase in electron density at the bridging atom leads to a decrease in the antiferromagnetic interaction. The tertiary alcohol bridges in $[\{CuL(NO_3)\}_2][NO_3]_2$ are considered more closely to resemble the hydroxy bridges in the compounds used to derive equation (4) than the *N*,*N*-dialkylated aminoalcohols used to derive the relationship (5), consistent with the 2*J* value obtained.

The ground-state magnetic orbitals in idealised trigonal-bipyramidal and square-based pyramidal geometries are d_{z^2} and $d_{x^2-y^2}$, respectively.[37] The intermediate co-ordination geometry of the two copper(II) ions in $[\{CuL(NO_3)\}_2][NO_3]_2$ leads to a low molecular symmetry of C_i, under which both the d_{z^2} and $d_{x^2-y^2}$ orbitals transform as A_{1g}, thus allowing orbital mixing. This scrambling of the d-orbital functions precludes a discussion of the mechanism of the ferromagnetic exchange in simple orbital pictures.

Acknowledgements

We would like to thank the SERC for a studentship (T. C. H.) and funding provided by the EC Human Capital and Mobility Framework III MASIMO Network. Drs. J. McMaster, R. Bhalla, D. Eardley and D. Collison are thanked for their valuable contributions.

References

1 O. Kahn, *Molecular Magnetism*, VCH, Weinheim, 1993, p. 161 and refs. therein.
2 P. J. Hay, J. C. Thibeault and R. Hoffmann, *J. Am. Chem. Soc.*, 1975, **97**, 4884.
3 V. H. Crawford, H. W. Richardson, J. R. Wasson, D. J. Hodgson and W. E. Hatfield, *Inorg. Chem.*, 1976, **15**, 2107.
4 H. E. LeMay, jun., D. J. Hodgson, P. Pruettiangkura and L. J. Theriot, *J. Chem. Soc., Dalton Trans.*, 1979, 781.
5 R. J. Butcher and E. Sinn, *Inorg. Chem.*, 1976, **15**, 1604 and refs. therein.
6 M. F. Charlot, O. Kahn, S. Jeannin and Y. Jeannin, *Inorg. Chem.*, 1980, **19**, 1410.
7 J. McMaster, R. Beddoes, D. Collison, D. R. Eardley, M. Helliwell and C. D. Garner, *Chem. Eur. J*, 1996, **2**, 685.
8 R. Bhalla, M. Helliwell and C. D. Garner, *Chem. Commun.*, 1996, 921; R. Bhalla, Ph.D. Thesis, University of Manchester, 1996.
9 T. C. Higgs, M. Helliwell and C. D. Garner, *J. Chem. Soc., Dalton Trans.*, 1996, 2101.
10 C. C. Tang, D. Davalian, P. Huang and R. Breslow, *J. Am. Chem. Soc.*, 1978, **100**, 3918.
11 R. Breslow, J. T. Hunt, R. Smiley and T. Tarnowski, *J. Am. Chem. Soc.*, 1983, **105**, 5337.
12 R. S. Brown and J. Huguet, *Can. J. Chem.*, 1980, **58**, 889.
13 F. E. Mabbs and D. Collison, *Electron Paramagnetic Resonance of d Transition Metal Compounds*, Elsevier, Amsterdam, 1992, ch. 16.
14 N. Walker and D. Stuart, *Acta Crystallogr., Sect. A*, 1983, **39**, 158.
15 C. J. Gilmore, MITHRIL, an integrated direct methods computer program, University of Glasgow, *J. Appl. Crystallogr.*, 1984, **17**, 42.
16 P. T. Beurskens, DIRDIF, Direct Methods for Difference Structures, an automatic procedure for phase extension and refinement of difference structure factors, Technical Report 1984/1, Crystallographic Laboratory, Toernooiveld, Nijmegen, 1984.
17 G. M. Sheldrick, SHELXS 86, in *Crystallographic Computing 3*, eds. G. M. Sheldrick, C. Kreuger and R. Goddard, Oxford University Press, 1985, p. 175.
18 (*a*) D. T. Cromer and J. T. Waber, *International Tables for X-Ray Crystallography*, Kynoch Press, Birmingham, 1974, vol. 4, Table 2.2A; (*b*) D. T. Cromer, *International Tables for X-Ray Crystallography*, Kynoch Press, Birmingham, 1974, vol. 4, Table 2.3.1.
19 C. K. Johnson, ORTEP, Report ORNL-5138, Oak Ridge Laboratory, Oak Ridge, TN, 1976.
20 G. J. Kleywegt, W. G. R. Wiesmeijer, G. J. Van Driel, W. L. Driessen, J. Reedijk and J. H. Noordik, *J. Chem. Soc., Dalton Trans.*, 1985, 2177.
21 (*a*) A. W. Addison, T. N. Rao, J. Reedijk, J. van Rijn and G. C. Verschoor, *J. Chem. Soc., Dalton Trans.*, 1984, 1349; (*b*) M. Zoeteman, E. Bouwman, R. A. G. de Graaff, W. L. Driessen, J. Reedijk and P. Zanello, *Inorg. Chem.*, 1990, **29**, 3487.
22 T. N. Sorrell, D. L. Jameson and C. J. O'Connor, *Inorg. Chem.*, 1984, **23**, 190.
23 E. Sinn, *Inorg. Chem.*, 1976, **15**, 366.
24 N. F. Curtis, G. R. Clark, B. W. Skelton and T. N. Waters, *J. Chem. Soc., Dalton Trans.*, 1977, 1051.
25 M. Andruh, O. Kahn, J. Sainton, Y. Dromzee and S. Jeannin, *Inorg. Chem.*, 1993, **32**, 1623.
26 A. Benzekri, P. Dubourdeaux, J.-M. Latour, J. Laugier and P. Rey, *Inorg. Chem.*, 1988, **27**, 3710.
27 C. J. O'Connor, D. Firmin, A. K. Pant, B. R. Babu and E. D. Stevens, *Inorg. Chem.*, 1986, **25**, 2300.
28 G. Speier, S. Tisza, Z. Tyeklár, C. W. Lange and C. G. Pierpont, *Inorg. Chem.*, 1994, **33**, 2041.
29 N. F. Curtis, F. W. B. Einstein, K. R. Morgan and A. C. Willis, *Inorg. Chem.*, 1985, **24**, 2026.
30 B. Chiari, J. H. Helms, O. Piovesana, T. Tarantelli and P. F. Zanazzi, *Inorg. Chem.*, 1986, **25**, 870.
31 L. Antolini, L. Menabue and M. Saladini, *Inorg. Chem.*, 1985, **24**, 1219.
32 N. A. Bailey, D. E. Fenton, J. R. Tate and P. M. Thomas, *J. Chem. Soc., Dalton Trans.*, 1985, 1471.
33 J.-P. Costes, F. Dahan and J.-P. Laurent, *Inorg. Chem.*, 1985, **24**, 1018.
34 F. E. Mabbs and D. Collison, *Electron Paramagnetic Resonance of d Transition Metal Compounds*, Elsevier, Amsterdam, 1992, ch. 15.
35 B. Bleaney and K. D. Bowers, *Proc. R. Soc. London, Ser. A*, 1952, **214**, 451.
36 L. Merz and W. Haase, *J. Chem. Soc., Dalton Trans.*, 1980, 875.
37 A. R. Rossi and R. Hoffmann, *Inorg. Chem.*, 1975, **14**, 365.

Received 24*th July* 1996; *Paper* 6/05180D